

**MAGNETOPHORETIC SEPARATION OF
MICROALGAE VIA IRON OXIDE
NANOPARTICLE**

TOH PEY YI

UNIVERSITI SAINS MALAYSIA

2015

**MAGNETOPHORETIC SEPARATION OF MICROALGAE VIA IRON
OXIDE NANOPARTICLE**

by

TOH PEY YI

Thesis submitted in fulfillment of the requirements

for the degree of

Doctor of Philosophy

August 2015

ACKNOWLEDGEMENT

First of all, I would like to express my heartiest gratitude to my supervisor, Dr. Derek Chan Juinn Chieh, Assoc. Prof. Dr. Lim Jit Kang and Prof. Dr. Abdul Latif bin Ahmad for their guidance and patience in leading me to complete my research. I deeply appreciate their invaluable advice, persistent encouragements, and financial support on the research in my PhD study.

Next, I would like to special thank my colleagues, especially Ng Bee Wah, Kong Li Peng, Yeap Swee Pin, Sum Jing Yao, Zeinab, Ngang Huey Ping, Chng Lee Muei, Khoo Chun Yu, Lim Guat Wei, Lim Jing Xiang, Chai Chuan Chun, and Nur Hidayah, who had given unselfishness sharing and help to me throughout my research. In addition, I wish to thank Chong Chi Han who was a former research assistant under this project.

Thanks to all the staffs, especially our respected Dean, Prof. Dr. Azlina bt. Harun @ Kamaruddin and Deputy Dean, Prof. Dr. Ahmad Zuhairi Abdullah, Assoc. Prof. Dr. Mohamad Zailani bin Abu Bakar and Assoc. Prof. Dr. Mohd Azmier Ahmad, all administrative staffs and technicians of School of Chemical Engineering, USM, and the technicians of EM Unit of School of Biological Science, USM, for their sincere help and support throughout my entire research work in USM.

I wish to show my gratitude to MyPhD scholarship for financial supporting me throughout my postgraduate study and the student research fund provided by USM through Postgraduate Research Grant Scheme (1001/PJKIMIA/8045037).

Last but not least, I wish to thank my beloved parents, Toh Hum Fah and Chai Kim, for their support and financial aid to complete my postgraduate study. Finally, I would like to thank my husband, Leong Wen Jia, for his moral support on me and his help on my parents. He had taken over my role as a daughter to help my parents when they get sick and face hardship during my study away from home. I am forever grateful.

Toh Pey Yi

August 2015

TABLE OF CONTENTS

Acknowledgement.....	ii
Table of Contents.....	iv
List of Tables.....	x
List of Figures.....	xii
List of Abbreviations.....	xix
List of Symbols.....	xxiii
Abstrak.....	xxvi
Abstract.....	xxviii

CHAPTER 1 - INTRODUCTION

1.1	Microalgae.....	1
1.2	Microalgal Biomass as Potential Feedstock for Biodiesel Production.....	2
1.3	Microalgae Blooming in Fishpond Water.....	3
1.4	Magnetophoretic Separation of Microalgae.....	4
1.5	Problem Statement.....	6
1.6	Research Objectives.....	9
1.7	Scope of Study.....	10
1.8	Organization of Thesis.....	11

CHAPTER 2 – LITERATURE REVIEW

2.1	Characteristic of Microalgae.....	14
2.1.1	Conventional Method on Microalgae Separation.....	16

2.1.2	Magnetophoretic Separation of Microalgae.....	17
2.1.2(a)	Interaction Mechanism.....	20
2.1.2(b)	XDLVO Analysis.....	25
2.2	Preparation of Magnetic Nanoparticles.....	29
2.2.1	Magnetic Nanoparticles.....	30
2.2.2	Surface Functionalization of Magnetic Nanoparticles	32
2.2.3	Cationic Polyelectrolyte.....	35
2.2.3(a)	Natural Cationic Polymer.....	37
2.2.3(b)	Synthetic Cationic Polymer.....	39
2.2.4	Colloidal Stability.....	40
2.3	Magnetic Separator.....	44
2.3.1	HGMS.....	45
2.3.2	LGMS.....	48
2.4	Biodiesel from Microalgae.....	52
2.4.1	Toxicity of Iron Oxide.....	53
2.4.2	Microalgal Biomass to Biodiesel.....	55
2.5	Summary.....	59

CHAPTER 3 - MATERIALS AND METHODS

3.1	The Flow of Experiments.....	61
3.2	Materials and Chemicals.....	62
3.3	Preparation and Characterization of IONPs.....	62
3.3.1	Bare-IONPs.....	62
3.3.2	SF-IONPs (PDDAvl).....	62
3.3.3	SF-IONPs (Chitosan).....	63

3.4	Colloidal Stability Measurement.....	64
3.5	Interaction Study of Particle-to-microalgal cell.....	66
3.5.1	Establishment and Characterization of Microalgal Cell...	66
3.5.2	Magnetophoretic Separation of Microalgae.....	67
3.5.2 (a)	Effect of pH on Surface Charge.....	67
3.5.2 (b)	Interaction Study on Particle-to-microalgal cell.....	67
3.5.2 (c)	Separation Kinetic.....	69
3.5.2 (d)	DLVO Modeling.....	70
3.6	Performance Study on Magnetophoretic Separation of Microalgae...	71
3.6.1	Study on the Colloidal Stability of SF-IONPs.....	72
3.6.1 (a)	Preparation of SF-IONPs with Different Dosage and MW of PDDA.....	72
3.6.1 (b)	Characterization of SF-IONPs.....	72
3.6.1 (c)	Performance of Magnetophoresis.....	73
3.6.2	Study on Different MW of PDDA.....	73
3.6.2 (a)	Preparation of SF-IONPs with Different MW of PDDA and Concentration.....	73
3.6.2 (b)	Performance of Magnetophoresis.....	74
3.6.3	Study on Different Concentration of SF-IONPs.....	74
3.6.4	Effect of Different Species of Microalgae.....	75
3.7	Feasibility Study on Biomass Harvesting Purpose.....	77
3.7.1	Ecotoxicity Study.....	77
3.7.2	Biodistribution of Magnetic Particles in Microalgal Cell..	78
3.7.3	Feasibility for Biodiesel Production.....	81

3.8	Case Study.....	82
3.8.1	Fishpond Water Sample.....	82
3.8.2	Continuous Biomass Harvesting.....	83
3.8.2 (a)	HGMS.....	84
3.8.2 (b)	LGMS.....	85
3.8.3	Reusability of Magnetic Particles.....	85
3.8.4	Cost Estimation.....	86

CHAPTER 4 - RESULTS AND DISCUSSIONS

4.1	Outline.....	88
4.2	Characterization of IONPs.....	89
4.2.1	Hydrodynamic Size Changes.....	89
4.2.2	Electrophoretic Mobility Measurement.....	90
4.2.3	Elemental Measurement and Magnetophoretic Behavior.....	91
4.2.4	Colloids Stability.....	92
4.3	Study on the Interaction Mechanism between IONPs and Freshwater <i>C. vulgaris</i>	94
4.3.1	Characterization of <i>C. vulgaris</i>	95
4.3.2	Particle-to-microalgal cell Attachment by ES Interaction.....	96
4.3.2 (a)	Isoelectric Point Determination.....	96
4.3.2 (b)	Performance of Magnetophoresis.....	99
4.3.2 (c)	SEM Verification.....	101
4.3.3	Separation Kinetic as a Function of Time.....	103
4.3.3 (a)	LDR-Setup Investigation.....	103
4.3.3 (b)	TEM Imaging.....	104

	4.3.3 (c)	Microscopy Imaging.....	107
4.3.4		DLVO Modeling.....	109
	4.3.4 (a)	Freshwater.....	100
	4.3.4 (b)	Seawater.....	120
	4.3.4 (c)	Ionic Strength Contribution.....	122
4.4		Performance Study of Magnetophoretic Separation of Microalgae...	126
	4.4.1	Colloidal Stability Contribution.....	126
		4.4.1 (a) Characteristic of SF-IONPs.....	127
		4.4.1 (b) Performance of Magnetophoresis.....	132
	4.4.2	Variation of Polyelectrolyte Molecular Weight.....	134
		4.4.2 (a) Characteristic of SF-IONPs.....	134
		4.4.2 (b) Performance of Magnetophoresis	134
	4.4.3	Particle Concentration.....	136
	4.4.4	Marine Microalgae.....	141
		4.4.4 (a) <i>Nannochloropsis</i> sp.	141
		4.4.4 (b) Bentic Diatom <i>Amphora</i> sp.	144
4.5		Feasibility Study on Magnetophoretic Separation of Microalgae for Biomass Harvesting.....	146
	4.5.1	Ecotoxicity of SF-IONPs (PDDAvl) on Growth of Microalgae.....	147
	4.5.2	Biodistribution of SF-IONPs (PDDAvl) in Microalgae....	151
	4.5.3	Feasibility of Biofuel Production.....	153
4.6		Case Study.....	154
	4.6.1	Feasibility of Microalgae Removal from Fishpond Water.	155
	4.6.2	Continuous Biomass Harvesting.....	158

4.6.2 (a)	HGMS.....	158
4.6.2 (b)	LGMS.....	160
4.6.3	Reusability of SF-IONPs.....	162
4.6.4	Cost Estimation.....	164
4.6.4 (a)	Fishpond Water Treatment Process.....	164
4.6.4 (b)	Biodiesel Production	168
CHAPTER 5 – CONCLUSION AND RECOMMEDATIONS		
5.1	Conclusion.....	172
5.2	Recommendations.....	174
REFERENCES.....		176
APPENDICES		
Appendix A		197
Appendix B		199
Appendix C		200
Appendix D		201
Appendix E		202
Appendix F		203
Appendix G.....		207
Appendix H.....		208
LIST OF PUBLICATIONS.....		211

LIST OF TABLES

		Page
Table 2.1	Cell separation performance in different case studied.	24
Table 2.2	Summary of the readily designed HGMS devices base on the magnetic induction, capacity, input power and manufacturer (Svoboda, 1987).	47
Table 3.1	The concentration of SF-IONPs stock that required to obtain respective dosage/concentration of SF-IONPs in cell medium with cell density at 3×10^7 cells/mL.	74
Table 3.2	The desired concentration of bare-IONPs/SF-IONPs (PDDAvl) stock that are required to obtain respective particle dosage in cell culture after mixing according to volume ratio of SF-IONPs (PDDAvl) to cell culture in 1:4.	77
Table 4.1	Hydrodynamic diameter of bare-IONPs and SF-IONPs in deionized water by Malvern Zetasizer Nano ZS. Results presented as average \pm standard deviation.	90
Table 4.2	Electrophoretic mobility measurement of the bare-IONPs and SF-IONPs in deionized water by Malvern Zetasizer Nano ZS. Results presented as average \pm standard deviation.	91
Table 4.3	Cell separation efficiency of <i>C. vulgaris</i> (3×10^7 cells/mL) at 300 mg/L of bare-IONPs and SF-IONPs (PDDAvl) for particle incubation duration of 1 min and 2 h. Cells are collected by LGMS with collection duration of 10 minutes. Results presented as average \pm standard deviation.	107
Table 4.4	Electrophoretic mobility of <i>C. vulgaris</i> cells, SF-IONPs (PDDAvl) and SF-IONPs-attached-cells. Results presented as average \pm standard deviation.	107
Table 4.5	Contact angle measurements of three different liquids on the surfaces of <i>C. vulgaris</i> , bare-IONPs, and SF-IONPs (PDDAvl). Results presented as average \pm standard deviation.	113
Table 4.6	Surface energy components and the interfacial energy of surface, <i>i</i> , with water and when surface <i>i</i> contact with each other in water medium.	115

Table 4.7	Detail on zeta-potential of each surface when dispersed in different medium condition together with pH. Results of zeta-potential presented as average \pm standard deviation.	121
Table 4.8	Zeta-potential and surface energy components of microalgae in seawater medium. Results of zeta-potential presented as average \pm standard deviation.	142
Table 4.9	Fatty acid methyl ester (FAME) content and yield of the oil extracted from the centrifuged biomass of <i>C. vulgaris</i> as a control and the SF-IONPs-attached-cells biomass collected from LGMS. Results presented as average \pm standard error.	154
Table 4.10	Cost estimation of fishpond water treatment when (a) LGMS and (b) HGMS applied in fishing farm of Aik Lee Fishery with 90% of cell separation efficiency for 300 mg/L and 50 mg/L of SF-IONPs (PDDAvI) respectively.	165
Table 4.11	The contribution of the SF-IONPs on the total cost when in different cell density culture in LGMS.	170

LIST OF FIGURES

		Page
Figure 1.1	Schematic flowchart of the scope of study.	11
Figure 2.1	Sketched M-H curves of (a) diamagnetic, (b) paramagnetic, (c) ferromagnetic, and (d) superparamagnetic particles (Pankhurst et al., 2003).	31
Figure 2.2	Schematic diagram of the synthesizing of graft copolymer reacting polyacrylic acid (PAA) with the amino-terminated polyethylene oxide (PEO-NH ₂) in temperature of 180 °C for 2 hours with continue flow of nitrogen gas.	33
Figure 2.3	Schematic diagram of the (a) synthesis of polymer-coated particle by grafting through photo-emulsionpolymerization and (b) the decomposition of the HMEM during photoinitiation (Guo et al., 1999).	34
Figure 2.4	Schematic image showed the charge neutralization effect from the electrostatic approach for flocculation of negative charge particles by cationic polyelectrolyte (Bolto and Gregory, 2007).	36
Figure 2.5	Schematic images of the phenomena of (a) bridging flocculation and (b) restabilisation from the steric effect (Bolto and Gregory, 2007).	37
Figure 2.6	Schematic design of a simple HGMS separator. (Hirschbein et al., 1982).	46
Figure 2.7	Schematic image of drum-type LGMS separator.	49
Figure 2.8	Biodiesel preparation from microalgal biomass through (M1) extraction and transesterification and (M2) direct transesterification (Adapted from Johnson and Wen, 2009b).	56
Figure 2.9	General overview of the transesterification reaction of triglyceride with methanol (Shi et al., 2012).	57
Figure 3.1	Schematic flowchart of the experimental works.	61
Figure 3.2	(a) Inhomogeneous magnetic field distribution across the medium contained in the custom cuvette for LGMS separation. (b) Schematic diagram of LDR setup employed in this study for data recording.	65

Figure 3.3	Schematic diagram showed the setup for the <i>C. vulgaris</i> cultivation in lab.	67
Figure 3.4	Image of vial (right) containing the water sample from the fishpond of Aik Lee Fishery fish farm (left).	83
Figure 3.5	Schematic diagrams of (a) HGMS and (b) LGMS setup in continuous mode of separation.	85
Figure 4.1	TEM image of bare-IONPs, Fe ₃ O ₄ (98+% purity, 20 – 30 nm) that was purchased from Nanostructured & Amorphous Materials, Inc.	90
Figure 4.2	XRD pattern of bare-IONPs. (Phase present: Magnetite, ICDD No.: 01-089-0691, 01-075-0449, and 00-003-0863; Maghemite, ICDD No.: 01-080-2186 and 01-089-5892).	92
Figure 4.3	Vibrating sample magnetometer-hysteresis loop data array for the bare-IONPs.	92
Figure 4.4	Sedimentation kinetic profile of the bare-IONPs and SF-IONPs colloidal suspension in function of time when in concentration of 133.33 mg/L.	93
Figure 4.5	The Hydrodynamic diameter of (a) bare-IONPs, (b) SF-IONPs (PDDAvI) and (c) SF-IONPs (Chitosan) at 0 s, 10 min, 3 h and 24 h. The nanoparticles dispersions are sonicated at 0s while the dispersion is re-suspended before each hydrodynamic size measurement by Malvern Zetasizer Nano ZS.	94
Figure 4.6	(a) Electrophoretic mobility of the <i>C. vulgaris</i> cells at different day of cultivation. (b) Growth curve of <i>C. vulgaris</i> . (c) The observed pH change of the cell culture medium with respect to cultivation day. Results presented as average ± standard deviation.	96
Figure 4.7	The electrophoretic mobility of <i>C. vulgaris</i> cells, bare-IONPs, SF-IONPs (PDDAvI) and SF-IONPs (Chitosan) in different pH condition. Results presented as average ± standard deviation.	98
Figure 4.8	Chemical structure of (a) PDDA and (b) the chitosan powder and the chitosan after the protonation in 1 wt% acetic acid solution.	99
Figure 4.9	Cell separation efficiency of 3×10^7 cells/mL <i>C. vulgaris</i> when mixed with 300 mg/L bare-IONPs and SF-IONPs through LGMS for 6 min of separation. Results of SF-IONPs presented as average ± standard deviation.	100

Figure 4.10	SEM micrograph of <i>C. vulgaris</i> cells from different collection method: (a) cells obtained from centrifugation, (b) cells obtained after exposure to polymer, (c) cells obtained after exposure to bare-IONPs collected via centrifugation, and (d) the cells collected from LGMS after mixed with the SF-IONPs.	102
Figure 4.11	(a) Quantitative curve for the kinetic separation of <i>C. vulgaris</i> (3×10^7 cells/mL) after added with 300 mg/L SF-IONPs (PDDAvI) in real time through LGMS for 20 minutes. Curve (ii) shows the lag stage of the magnetophoretic separation that occurred in first few second. (b) Image observation of the real time magnetophoretic separation of <i>C. vulgaris</i> after addition of 300 mg/L SF-IONPs.	104
Figure 4.12	TEM images of (a) bare-IONPs, (b) <i>C. vulgaris</i> cell when mixed with bare-IONPs, (c) SF-IONPs-attached-cells, and the flocculation of SF-IONPs-attached-cells (d and e) without and (f) with magnet is introduced.	106
Figure 4.13	Figure shows the kinetic separation curve of the <i>C. vulgaris</i> cells added with 300 mg/L of SF-IONPs (PDDAvI) in function of separation time together with the microscopy images that shows the morphology of the flocculated clusters in real time and also the sample images.	108
Figure 4.14	Schematic shows the parameters of the distance between the surfaces of cell and magnetic nanoparticles, d ; the radius of magnetic nanoparticles, R ; and the thickness of the polymer adlayer that coated on magnetic nanoparticle surface, δ , which used in DLVO modelling.	112
Figure 4.15	Overall interacting potential between <i>C. vulgaris</i> cells and (a) bare-IONPs and (b) SF-IONPs (PDDAvI) based upon XDLVO analysis in freshwater.	117
Figure 4.16	Zeta-potential of <i>C. vulgaris</i> , bare-IONPs and SF-IONPs (PDDAvI) in function of pH.	118
Figure 4.17	Diagrams show the U_{ES} curve as a function of distance between <i>C. vulgaris</i> and (a) bare-IONPs and (b) SF-IONPs (PDDAvI) at different pH condition.	119

Figure 4.18	Diagrams show the (a) well depth of secondary minimum predicted by the XDLVO analysis and the (b) cell separation efficiency from experiment observation when the <i>C. vulgaris</i> cells are interacting with the bare-IONPs and SF-IONPs (PDDAvl) at different pH.	119
Figure 4.19	Microscopic images on the attachment of <i>C. vulgaris</i> cells after mixed with the (a) bare-IONPs and (b) SF-IONPs in seawater condition. (Magnification: 100x)	120
Figure 4.20	Overall interacting potential between <i>C. vulgaris</i> Cells and (a) bare-IONPs and (b) SF-IONPs (PDDAvl) based upon XDLVO analysis in seawater.	122
Figure 4.21	Cell separation efficiency of <i>C. vulgaris</i> in function of NaCl concentration up to 700 mM, which is equivalent to the ionic strength of seawater. Results presented as average \pm standard deviation.	123
Figure 4.22	(a) XDLVO analysis of the net interaction between the <i>C. vulgaris</i> cells and SF-IONPs (PDDAvl) at different NaCl concentration. (b) Well depth of the secondary minimum predicted by the XDLVO in function of NaCl concentration calculated from (a).	124
Figure 4.23	The normalized interaction potential of (a) ES and (b) AB interaction with respect to the separation distance, d between <i>C. vulgaris</i> and SF-IONPs (PDDAvl) at difference NaCl concentration.	125
Figure 4.24	Zeta potential of <i>C. vulgaris</i> and SF-IONPs (PDDAvl) with respect to the concentration of NaCl. Results presented as average \pm standard deviation.	126
Figure 4.25	(a) Electrophoretic mobility and (b) hydrodynamic diameter of SF-IONPs coated with different MW PDDA in respective optimum dosage of polymer, which is 100 g/g PDDA for SF-IONPs (PDDAvl), SF-IONPs (PDDAl) and SF-IONPs (PDDAm), and 50 g/g for SF-IONPs (PDDAh). Results presented as average \pm standard deviation.	128
Figure 4.26	Schematic diagram illustrates the possible polymer conformation on the SF-IONPs: (a) flat conformation and extended conformation that dominated by (b) loops and tails, and (c) tails.	130

Figure 4.27	Figure shows the sedimentation kinetic profile of the SF-IONPs colloidal suspension in function of time for 133.33 mg/L of (a) SF-IONPs (PDDAvl) coated by different dosage of PDDAvl and (b) SF-IONPs coated by different MW of PDDA with respective optimum polymer dosage.	131
Figure 4.28	Cell separation efficiency of <i>C. vulgaris</i> cells (3×10^7 cell/mL) by using 133.33 mg/L of SF-IONPs that prepared by different MW and dosage of PDDA through LGMS for 6 min. Results presented as average \pm standard deviation.	133
Figure 4.29	Cell separation efficiency of the <i>C. vulgaris</i> (3×10^7 cells/mL) in different concentration of SF-IONPs that has coated by different MW of PDDA. Results presented as average \pm standard deviation.	135
Figure 4.30	Kinetic curve of the separation efficiency as the function of time when different concentration of SF-IONPs (PDDAvl) is used for <i>C. vulgaris</i> cell separation in LGMS.	136
Figure 4.31	(a) Separation time of SF-IONPs-attached-cells to achieve maximum separation efficiency and (b) initial separation rate of SF-IONPs-attached-cells in first 39 s with respect to the concentration of SF-IONPs (PDDAvl).	138
Figure 4.32	Microscopic images showing the size of the SF-IONPs-attached-cells cluster after the induced-aggregation by the NdFeB permanent magnet for 5 s when different concentration of SF-IONPs (PDDAvl) is added to <i>C. vulgaris</i> media. (Magnification: 100x)	140
Figure 4.33	(a) XDLVO analysis for the interaction between the marine species <i>Nannochloropsis</i> sp. with bare-IONPs and SF-IONPs (PDDAvl). Results presented as average \pm standard deviation.	142
Figure 4.34	Microscopic image of <i>Amphora</i> sp. that contains EPS as shown by the arrow. (Magnification: 100x)	144
Figure 4.35	(a) XDLVO analysis for the interaction between the benthic diatom <i>Amphora</i> sp. with bare-IONPs and SF-IONPs (PDDAvl). (b) Cell separation efficiency of <i>Amphora</i> sp. under LGMS at different dosage. Results presented as average \pm standard deviation.	145
Figure 4.36	Cell density of <i>C. vulgaris</i> that exposed to different dosage of SF-IONPs (PDDAvl) in the culture medium. Results presented as average \pm standard error.	148

Figure 4.37	Total lipid yield of the <i>C. vulgaris</i> biomass at day 7 th after growing in medium that containing different dosage of SF-IONPs (PDDAv1). ANOVA analysis ($P < 0.05$) was represented by the attached alphabet. Results presented as average \pm standard error.	149
Figure 4.38	Microscopic images show the <i>C. vulgaris</i> cells in culture medium at day 7 th for the control and in 20 mg/L of SF-IONPs (PDDAv1). (Magnification: 100x)	149
Figure 4.39	The inhibition effect on the growth of <i>C. vulgaris</i> based on cell density inhibition compared to the control with respect to the day of cultivation when in dosage of 32 g SF-IONPs/g dry biomass (Appendix G). Results presented as average \pm standard error.	150
Figure 4.40	TEM micrographs show the images of the cross-sectional view of <i>C. vulgaris</i> cell attached with the SF-IONPs (PDDAv1) collected from LGMS.	152
Figure 4.41	Cell separation efficiency of microalgae from fishpond water as a function of SF-IONPs (PDDAv1) concentration. Images of the sample (bottom) are attached together. Results presented as average \pm standard deviation.	156
Figure 4.42	Cell separation efficiency of <i>C. vulgaris</i> (3×10^7 cells/mL) after mixing with different concentration of SF-IONPs (PDDAv1) through the continuous mode HGMS in flow rate of 1.25 mL/min. Results presented as average \pm standard deviation.	160
Figure 4.43	Cell separation efficiency of <i>C. vulgaris</i> (3×10^7 cells/mL) after added with different concentration of SF-IONPs (PDDAv1) through the continuous mode LGMS in flow rate of 1.25 mL/min. Results presented as average \pm standard deviation.	161
Figure 4.44	Detachment efficiency of <i>C. vulgaris</i> cells from the SF-IONPs-attached-cells biomass in different ionic strength condition that induced by different valence of salt.	163
Figure 4.45	Block flow diagram of the magnetophoretic separation of microalgae from fishpond water for water purification purpose.	164

Figure 4.46	Cell separation efficiency of the microalgal cells from the fishpond water through LGMS and HGMS as a function of SF-IONPs (PDDAvI) concentration. Results presented as average \pm standard deviation.	167
Figure 4.47	Estimated price of algal oil as a function of microalgal culture cell density in range of 1 g/L to 10 g/L in different oil content by the LGMS.	170

LIST OF ABBREVIATIONS

AB	Lewis acid-base interaction
AlCl ₃	Aluminum chloride
Al ₂ O ₃	Aluminum oxide
Al ₂ (SO ₄) ₃ •18H ₂ O	Aluminum sulfate
ANOVA	Statistical analysis by one-way analysis of variance
APTES	(3-aminopropyl)triethoxysilane
Bare-IONPs	Bare iron oxide nanoparticles
BBM	Bold's Basal Medium
C16:0	Palmitic acid
C18:2	Linoleic acid
CaCl ₂	Calcium chloride
CaO/Al ₂ O ₃	Alumina supported calcium oxide
CATCS	Cationic crosslinking-copolymer
CMC-g-PDMC	Carboxymethyl chitosan-graft-poly[(2-methacryloyloxyethyl) trimethyl ammonium chloride]
CO ₂	Carbon dioxide
COD	Chemical oxygen demand
CuO	Copper oxide
DEAE	Diethylaminoethyl
DLVO	Derjaguin-Landau-Verwey-Overbeek
DMC	(2-methacryloyloxyethyl) trimethyl ammonium chloride
DNA	Deoxyribonucleic acid
DUFA	Di-unsaturated fatty acids
EPS	Extracellular polymeric substance

ES	Electrostatic
FAME	Fatty acid methyl ester
FeCl ₃	Ferric chloride
FFA	Free fatty acid
GCMS	Gas chromatography mass spectrometer
HCl	Hydrochloric acid
HGMF	High gradient magnetic filtration separator
HGMS	High gradient magnetophoretic separation
HMEM	2-[p-(2-hydroxy-2-methylpropiophenone)]-ethylene glycol-methacrylate
ICDD	International Centre for Diffraction Data
IO	Iron oxide
IONPs	Iron oxide magnetic nanoparticles
KCl	Potassium chloride
LDR	Light dependent resistor
LDR setup	Optical light intensity sensing system
LGMS	Low gradient magnetophoretic separation
LSD	Least significant different
Mg ²⁺	Magnesium
MRI	Magnetic resonance imaging
MUFA	Mono-unsaturated fatty acids
MW	Molecular weight
NaCl	Sodium chloride
NaOH	Sodium hydroxide
NdFeB	N50-graded neodymium boron ferrite

NSF	National Sanitation Foundation
PAA	Polyacrylic acid
PAM	Polyacrylamide
PDDA	Poly(diallyldimethylammonium chloride)
PDDAh	High molecular weight poly(diallyldimethylammonium chloride)
PDDAl	Low molecular weight poly(diallyldimethylammonium chloride)
PDDAm	Medium molecular weight poly(diallyldimethylammonium chloride)
PDDAvl	Very low molecular weight poly(diallyldimethylammonium chloride)
PEI	Polyethylenimine
PEO	Polyethylene oxide
PEO-NH ₂	Amino-terminated polyethylene oxide
PS	Polystyrene
PSS70k	Poly(styrene sulfonate) with molecular weight of 70,000 g/mol
PSS1000k	Poly(styrene sulfonate) with molecular weight of 1000,000 g/mol
PUFA	Poly-unsaturated fatty acids
ROS	Reactive oxygen species
SEM	Scanning Electron Microscope
SF-IONPs	Surface functionalized iron oxide nanoparticles
SF-IONPs (Chitosan)	SF-IONPs coated with chitosan
SF-IONPs (PDDA)	SF-IONPs coated with PDDA
SF-IONPs (PDDAh)	SF-IONPs coated with PDDAh
SF-IONPs (PDDAl)	SF-IONPs coated with PDDAl

SF-IONPs (PDDAm)	SF-IONPs coated with PDDAm
SF-IONPS (PDDAvl)	SF-IONPs coated with PDDAvl
SiO ₂	Silica
TEM	Transmission Electron Microscope
TiO ₂	Titanium oxide
UFA	Unsaturated fatty acid
vdW	van der Waals
VSM	Vibrating sample magnetometer
XDLVO	Extended Derjaguin-Landau-Vewey-Overbeek
XRD	X-ray diffraction

LIST OF SYMBOLS

A_{eff}	Effective Hamaker constant
A_i	Hamaker constant of material i
B	Magnetic induction
∇B	Magnetic field gradient
C	Hydrodynamic fiction coefficient
$C_{\text{algal oil}}$	Price of microalgal oil in \$/L
$C_{\text{petroleum}}$	Price of crude oil in \$/bbl
d	Surface-to-surface separation distance between the cell and the IONP
d_0	Minimum equilibrium distance between two condensed-phase surfaces
E_{kinetic}	Translational kinetic energy
F_{drag}	Drag force
F_{mag}	Magnetic force
$\Delta G_{iwi}^{\text{AB}}$	AB interfacial interaction energy between material i and i in water
$\Delta G_{ijw}^{\text{AB}}$	AB interfacial interaction energy between material i and j in water
H	Magnetic field
$I_{\text{centrifuged}}$	Absorbance intensity of the clear centrifuged sample
I_{DW}	Absorbance intensity of the clear distilled water
I_0	Absorbance intensity of initial microalgal suspension
$I(t)$	Absorbance intensity of microalgal suspension during magnetophoretic separation at time t
M	Magnetization
R	Radius of IONP

U_{AB}	Interacting potential of Lewis acid-base interaction
U_{DLVO}	Total interacting potential (estimated by DLVO analysis)
U_{ES}	Interacting potential of electrostatic interaction
u_{mag}	Magnetophoretic velocity
U_{mag}	Interacting potential of magnetic interaction
U_{steric}	Interacting potential of steric interaction
U_{vdW}	Interacting potential of van der Waals interaction
U_{XDLVO}	Total interacting potential (estimated by XDLVO analysis)
V	Volume
$V_{centrifuged}$	Voltage recorded of the clear centrifuged sample
V'_f	Voltage recorded of the clear medium
V_{mag}	Volume of SF-IONPs
V_0	Voltage recorded of initial microalgal suspension
V'_0	Voltage recorded of initial particle suspension
$V(t)$	Voltage recorded of microalgal suspension during magnetophoretic separation at time t
$V'(t)$	Voltage recorded of particle suspension during sedimentation at time t

Greek Letters

γ	Surface tension
γ^{\oplus}	Electron acceptor surface tension parameter
γ^{\ominus}	Electron donor surface tension parameter
γ_i^{LW}	The vdW component of the material surface tension
ξ	Zeta-potential
κ	Debye-Hückel parameter
ϵ_r	Relative permittivity of water
ϵ_0	Permittivity of free space
δ	Adlayer thickness
λ	Correlation length of molecule in a liquid medium
Σ	Total amount

PEMISAHAN MIKROALGA DENGAN PEMISAHAN BERMAGNET MELALUI NANO ZARAH FERUM OKSIDA

ABSTRAK

Penuaian mikroalga adalah penting untuk mengumpul biojisim mikroalga sebagai bahan mentah bahan api bio dan untuk mengelakkan pencemaran air sekunder yang disebabkan oleh penguraian biojisim mikroalga dalam air. Pemisahan mikroalga dengan pemisahan bermagnet telah diiktiraf sebagai kaedah boleh laksana untuk menuai mikroalga. Ia dilakukan melalui pelekatan nano zarah ferum oksida (IONPs) pada permukaan sel untuk memberikan sifat bermagnet terhadap sel-sel dan seterusnya membolehkan pengumpulan sel dengan menggunakan magnet kekal. Mekanisme elektrostatik-pengantara-pelekatan yang membolehkan pelekatan dan penanggalan zarah-pada-sel mikroalga biasanya dilakukan melalui penyelarasan pH. Walau bagaimanapun, keperluan penyelarasan pH pada media pengkulturan mikroalga menghalangnya daripada diaplikasi pada berskala besar. Oleh itu, kaedah perfungsi pada permukaan IONPs untuk membentuk permukaan berfungsi IONPs (SF-IONPs) yang bercas positif perlu dilakukan untuk mengatasi kelemahan penyelarasan pH. Penyelidikan ini merangkumi pencirian SF-IONPs, pemodelan interaksi zarah-pada-sel mikroalga, kinetik pemisahan dalam pemisahan bermagnet berkecerunan rendah (LGMS), dan kebolehlaksanaannya pada rawatan air dan penghasilan bahan api bio. SF-IONPs yang stabil dan bercas positif yang telah disediakan melalui kaedah “immobilized-on” boleh melekat pada *Chlorella vulgaris* air tawar melalui tarikan elektrostatik (ES). Permukaan perfungsi menggunakan poli(diallyldimethylammonium klorida) (PDDA) dipilih daripada kitosan disebabkan

cas permukaannya tidak bergantung pada pH. Kecekapan pemisahan sel yang tinggi iaitu >97% telah diperolehi dalam semua julat pH yang diuji dan kualiti minyak daripada biojisim tidak terjejas. Kajian kinetik menunjukkan bahawa pemisahan sel melalui LGMS ($\nabla B < 80$ T/m) dimulai oleh pengagregatan zarah-pada-sel mikroalga semasa pengeraman dan diikuti oleh medan-teraruh-pengagregatan di bawah medan magnet. Analisis Extended Derjaguin-Landau-Vewey-Overbeek (XDLVO) telah digunakan untuk meramal interaksi di antara SF-IONPs dan sel mikroalga dengan mengambil kira interaksi van der Waals (vdW), ES dan Lewis asid-bes (AB). Interaksi ES didapati menentukan hasil interaksi di antara sel dan SF-IONPs dalam media air tawar manakala interaksi AB dan vdW memainkan peranan dominan dalam air laut. XDLVO meramalkan pelekatan SF-IONPs pada permukaan sel adalah berkesan dengan minimum sekunder sebanyak -3.12 kT, di mana ia selaras dengan keputusan eksperimen. Ini memberikan pemahaman mengenai strategi penanggalan zarah daripada sel supaya diguna semula. Secara keseluruhannya, prestasi SF-IONPs amat bergantung pada kestabilan zarah, berat molekul (MW) PDDA, kepekatan zarah, dan spesis alga. SF-IONPs yang disalut oleh PDDA yang MW sangat rendah pada dos 100 g PDDA/g IONPs membentuk ampaiian yang paling stabil dan ia membolehkan pemisahan *C. vulgaris* menghampiri 100% dengan kepekatan SF-IONPs ≥ 50 mg/L. Kesan teduhan cahaya dan aglomerasi cel adalah kesan utama yang menyebabkan SF-IONPs (PDDA_{v1}) toksik terhadap pertumbuhan *C. vulgaris*. Teknologi ini telah terbukti berkesan dan mencapai kos munasabah dalam rawatan air kolam ikan. Kecekapan pemisahan sel sebanyak 90% telah dicapai dan juga kos rawatan air sebanyak USD\$ $0.15/m^3$ dengan dos 0.519 g SF-IONPs/g biojisim kering melalui LGMS. Dalam penghasilan bahan api bio, penambahbaikan diperlukan untuk memenuhi kebolehlaksanaan ekonomi.

MAGNETOPHORETIC SEPARATION OF MICROALGAE VIA IRON OXIDE NANOPARTICLE

ABSTRACT

Harvesting of microalgae biomass is a crucial step in obtaining the microalgae biomass as biofuel feedstock and also to avoid the secondary water pollution caused by the decomposition of microalgae biomass in the water system. Magnetophoretic separation is being recognized as a feasible method to harvest the microalgae. It is performed via attachment of iron oxide magnetic nanoparticles (IONPs) on the cell surface in order to impart the magnetic property onto the cells and hence enable the subsequent collection of cells by using a permanent magnet. The electrostatic-mediated-attachment mechanism which enables the attachment and detachment of particle-to-microalgal cell is usually done through a series of pH manipulation. However, the need of pH adjustment onto the microalgae culture medium prohibited the use of this technology in large scale application. Therefore, the surface functionalization of IONPs to form positively charged surface functionalized IONPs (SF-IONPs) is carried out in order to overcome the drawback associated with pH manipulation. This study looked into the characterization of the prepared SF-IONPs, the modeling of particle-to-microalgal cell interaction, the separation kinetic in low gradient magnetic separation (LGMS), and its feasibility on water treatment and biofuel production. The colloidally stable positively charged SF-IONPs which were prepared via immobilized-on approach promote effective electrostatic attachment of SF-IONPs on the freshwater *Chlorella vulgaris*. The surface functionalization using poly(diallyldimethylammonium chloride) (PDDA)

was chosen over chitosan since its surface charge are not pH dependent. A high cell separation efficiency of > 97 % was obtained in all range of pH tested and the oil quality from the harvested biomass was not affected. The kinetic study indicated that the cell separation is initiated via particle-to-microalgal cell aggregation during incubation followed by field-induced-aggregation under magnetic field in LGMS with $\nabla B < 80$ T/m. Extended Derjaguin-Landau-Vewey-Overbeek (XDLVO) analysis employed to predict the interaction between SF-IONPs and microalgal cells took into account the van der Waals (vdW), ES and Lewis acid-base (AB) interactions. The ES interaction governed the net interaction between cell and SF-IONPs in freshwater media while the AB and vdW interactions play a dominant role in seawater. XDLVO predicted effective attachment of SF-IONPs onto cell surface with a secondary minimum of -3.12 kT, which is in accordance with the experimental result. This gave an insight on the strategy of particle detachment from cell for reuse. In overall, the performance of SF-IONPs is strongly depending on the particle stability, molecular weight (MW) of PDDA, particle concentration, and the microalgae species. The SF-IONPs coated by very low MW PDDA at dosage of 100 g PDDA/g IONPs formed the most colloiddally stable suspension and it enabled the separation of *C. vulgaris* at almost 100 % efficiency with SF-IONPs concentration of ≥ 50 mg/L. The light shading effect and cell agglomeration were the main toxic effect of SF-IONPs (PDDA_{vl}) toward the growth of *C. vulgaris*. This technology was proven effective and cost feasible in fishpond water treatment. A cell separation efficiency of 90 % was achieved and at water treatment cost of USD\$0.15/m³ with a dosage of 0.519 g SF-IONPs/g dry biomass under the LGMS. In biofuel production, further improvement is required to meet the economic feasibility.

CHAPTER ONE

INTRODUCTION

1.1 Microalgae

Microalgae are unicellular species microscopic algae, which exist individually in chains or in groups and are typically found in both freshwater and marine systems (Demirbas, 2010). They do not have roots, stems and leaves (Brennan and Owende, 2010). They convert the sunlight, water and carbon dioxide to algal biomass (Demirbas, 2010). Since the structures of algae are primarily for energy conversion without any development beyond complex cellular structure, so they are able to adapt to prevailing environmental conditions and prosper in the long term (Brennan and Owende, 2010).

Microalgae are in micron-size, which cause them very difficult to be collected physically. However, microalgal cell surface are always in net negatively charged because of the present of lipids, proteins and sugars, which have functional groups like $-SH$, $-OH$ and $-COOH$. Deprotonation of those ligands will give a net negative charge on cell surface at natural water medium (Molina-Grima et al., 2003; McLaughlin and Poo, 1981; Gadd, 2009). The microalgal cells tend to repel each other by the electrostatic repulsion force. Hence, they form a quite stable cell suspension in the growing medium and cause very slow cell sedimentation (Vandamme et al., 2013). Moreover, the low amount of biomass in huge amount of growing medium (with only up to 1 g/L for open pond culture system) makes the cell harvesting tremendously challenging (Pulz, 2011; Vandamme et al., 2013).

1.2 Microalgal Biomass as Potential Feedstock for Biodiesel Production

The energy crisis has ignited the search of an alternative replacement for fossil fuel which can be more environmental friendly and sustainable. Since the microalgae biomass is capable of producing high oil yield up to 14 641 gallons per acre basis in up to two orders of magnitude higher than other oil producer crops (Johnson, 2009), it makes microalgae an attractive option to combat the energy crisis (Stephens et al., 2010; Ahmad et al., 2011a). The renewable fuel source from microalgae is limitless as its energy source is from the sun itself via photosynthesis (Demirbas, 2010). During phototrophic cultivation, microalgae need sunlight and intake carbon dioxide (CO₂) as carbon source. Besides that, it also consumes inorganic elements that constitute the cells. Therefore, it can grow in the nutrient rich water broth that unsuitable for human consumption. During the growth of microalgae, the consumption of nutrients by microalgae has contributed to the wastewater treatment too (Mata et al., 2010). The carbon contained in microalgal biomass is typically derived from carbon dioxide (CO₂), where about 183 t of CO₂ has been fixed with each 100 t of biomass. In order to transform the biomass into the biofuels, thermochemical transformation such as liquefaction, pyrolysis and gasification are able to generate gases, liquids and solid fuels while biochemical process can be used to produce the bioethanol, biodiesel and bio-hydrogen (Demirbas, 2010; and Huang et al., 2010).

It is predicted that biofuel production technology based on microalgae could reach maturity stage within another 10 to 15 years (Wijffels and Barbosa, 2010). However, the main restriction in preventing the realization for large-scale third generation microalgal oil production is the high harvesting cost of microalgae

biomass. The cost associated to downstream separation processes could reach up to 20–30% of the total production cost of biomass (Grima et al., 2003).

1.3 Microalgae Blooming in Fishpond Water

In man-made environment, microalgae biomass are abundantly encounter in aquaculture and freshwater fisheries due to the seasonal blooms as the water rich in nutrients which originated from the fish excretion, excess fish food and decaying organic matter (Huang et al., 2010; Perez-Garcia et al., 2011). Most of those nutrients promote the growth of microalgae are in organic matter form and they can be quantified as Chemical Oxygen Demand (COD) with an ideal value for fishpond at less than 50 mg/L (Santhosh and Singh, 2007). Ironically, the growth of the microalgae naturally is beneficial for the removal of the excess nutrient in the water to avoid nutrient overloading as well as reducing the COD level. However, this benefit is diminished once the microalgae start to grow excessively. For a typical freshwater fishpond, the microalgae will constantly grow as long as there are nutrient to substantiate its growth. High microalgae concentration is beneficial as oxygen source through photosynthesis and also provides shades for fishes from the sunlight (Dermibas, 2010). However, the high concentration of microalgae will be disastrous, as their huge amount will exhaust the oxygen supply through respiration and releasing carbon dioxide during nighttime. Fish may be killed overnight through suffocation (NT Fisheries Group, 2004) when dissolved oxygen (DO) is less than 2 mg/L (Kangur et al., 2005). In most cases, DO in fish pond should be maintained at least 4 mg/L all the time (Santhosh and Singh, 2007). At extreme high nutrient level eutrophication will occur (Kangur et al., 2005). The nutrient will promote excessive growth of algae bloom in the presence of sunlight. The sunlight will be blocked

totally by the dense algae bloom to form a death zone beneath the bloom with drastic oxygen depletion and hence deteriorate the fish production.

Conventionally, there are multiple well-practiced methods to maintain the microalgae population within a small fishpond (Borics et al., 2000). Effective management of microalgae growth can be achieved naturally via few methods, such as, growing aquatic plants around the fishpond to consume the nutrient and starving the microalgae (Crites et al., 1988; Wolverton, 1988), avoid over feeding and using high quality food to ensure complete digestion of the food (Masser et al., 1992), and using barley straw to control algae growth in pond (Graslund and Bengtsson, 2001). Besides the natural treatment, by using the algacides chemical, which contain simazine, chelated copper and potassium permanganate, is also able to kill the algae but it is harmful to living organisms and environment (Graslund and Bengtsson, 2001). The quick death of all the microalgae may increase ammonium concentration and decrease dissolve oxygen in water and hence it is not favorable. Nevertheless, most of the standard practices involved for microalgae removal were labor intensive and had limited efficiency (Weijerman et al., 2008). Since microalgae biomass can be employed as third generation biofuel (Cheng et al., 2009) and other useful products, like nutrients in form of polyunsaturated fatty acid (PUFA) (Wen and Chen, 2003; Ward and Singh, 2005; Brennan and Owende, 2010) or pigment (Borowitzka, 1999; Curtain, 2000). Therefore, a robust removal technique without direct annihilation of microalgae will be economically more attractive.

1.4 Magnetophoretic Separation of Microalgae

Magnetophoretic separation of microalgae has been introduced in 1970s (Yadida et al., 1977; Bitton et al., 1975) and it was revisited recently by numerous

researchers due to the potential applications derived from their microalgae biomass as biofuel feedstock (Liu et al., 2009; Xu et al., 2011; Cerff et al., 2012; Hu et al., 2013; Prochazkova et al., 2013; Liu and Zhang, 2009; Wang et al., 2013b; Lee et al., 2013; Hu et al., 2014a; Seo et al., 2014). There are few conventional microalgae separation methods have been developed to meet high microalgae separation efficiency, which are filtration, centrifugation, and flocculation and settling (Hoffmann, 1998; Molina-Grima et al., 2003). Due to the drawback of the high energy consumption, time consuming and costly conventional methods, the new advancement in microalgae separation method via magnetophoretic separation are envisaged to be able to overcome the weakness. This method of microalgae separation is far more affirmative than that of the conventional separation method for high throughput processing and biomass harvesting. It is one of the most promising approaches for harvesting microalgae due to its attractive advantages such as (1) high throughput, (2) less energy intensive, (3) high separation efficiency, and (4) flexible for implementation and scalability (Zborowski et al., 2002; Bucak et al., 2011; Prochazkova, et al., 2013).

The underlying working principle for the magnetophoretic separation technique is straightforward. It centers on the need to tag non-magnetic microalgal cells with iron oxide magnetic nanoparticles (IONPs). The tagged biomass is then exposed to an externally applied magnetic field to achieve its separation. Even though this method is being actively discussed currently but there is still lack of proper understanding of working concept due to the limited fundamental knowledge about this method. Therefore, fundamental and bioengineering study onto this method of magnetophoretic separation of microalgae should be carefully explored in

order to consolidate the basis information of this technology for future research and development.

1.5 Problem Statement

The method of magnetophoretic separation of microalgae was first introduced in the mid 1970s in order to remove the harmful microalgae from the pond and lake (Bitton et al., 1975; Yadida et al., 1977). After a long gap of about 30 years, this separation method is revisited and it has been widely investigated from different perspective due to its advantages for microalgae biomass recovery. This method was proven effective in harvesting microalgae from freshwater as well as seawater medium (Cerff et al., 2012). Among all the studies, there are two mechanism were utilized to impart the magnetic property on the freshwater microalgal cells: namely, (i) electrostatic-mediated-attachment (Xu et al., 2011; Liu et al., 2009; Prochazkova et al., 2012; Lee et al., 2013; Seo et al., 2014) and (ii) adsorption-based-attachment (Cerff et al., 2012; Hu et al., 2013). From the studies that utilized the adsorption-based-attachment mechanism, there was no discovery on the proper way to recover the magnetic particle from the harvested biomass. Although Xu and coworkers (2011) had proven that the magnetic nanoparticles can be regenerated by using the hydrochloric acid to dissolve the magnetic nanoparticles, but this method was not applicable for every species of microalgae due to the problem of cell leakage in high acidic condition (Xu et al., 2011). While for the mechanism of electrostatic-mediated-attachment, the effective attachment and detachment of particle-to-microalgal cell are predictable and controllable by using the technique of pH adjustment (Prochazkova et al., 2013; Seo et al., 2014). Therefore, the mechanism of

electrostatic-mediated-attachment was seen more promise and practical for the magnetophoretic separation of microalgae.

From the study of Xu et al., (2011) and Prochazkova et al., (2013), they verified that the magnetic particles was able to attach on cell surface by the mechanism of electrostatic-mediated-attachment through a series of pH adjustment. However when the magnetic particles are having an isoelectric point lower than the pH of the natural cell culture medium, it tends to cause the magnetophoretic separation of microalgae become impractical for real environmental application. For example in natural freshwater microalgae culture with pH range from pH 7 to pH 9, the microalgal cells always maintain their net negative charge while the magnetic particles that has an isoelectric point lower than the pH value of cell culture will be in negatively charged too (Hu et al., 2013; Prochazkova et al., 2013). The similar negatively charged surfaces tend to repel each other due to electrostatic repulsion. In order to induce the effective attachment of particle-to-microalgal cell, the pH of the microalgae medium must be adjusted to a lower pH value than the isoelectric point of magnetic particles so that the magnetic particles become positively charged to induce attachment on cells (Prochazkova et al., 2013). Even though the cell separation can be performed efficiently but the treated water has become acidic which cannot be reused for aquaculture purpose and tend to cause water pollution if discharge to the surrounding. Therefore, the pH adjustment strategy is impractical for the implementation of magnetophoretic separation for engineering application.

From another perspective, the use of magnetic particles had enabled the direct recovery of the magnetic particles from the harvested biomass through charge reversal around its isoelectric point. The magnetic particles can be detach from the particle-crowded-biomass, up to 90 % of detachment efficiency, by increase the pH

to pH12 so that the magnetic particles become negative charge again and tend to repel/detach from the cells (Prochazkova et al., 2013; Seo et al., 2014). Even though the pH adjustment was quite effective for magnetophoretic separation of microalgae in terms of attachment and detachment, but this method has the risk of causing cell lysis (Surendhiran and Vijay, 2014; Udhaya et al., 2014) in addition the water is required to be treated again before discharge to the environment. Therefore, another different surface property of magnetic material should be designed in order to cope with the weakness as mentioned above.

Even though the method of magnetophoretic separation of microalgae has been investigated since 2009, but it still lack of fundamental study onto the effective interaction and the bioengineering study onto the biomass harvested. Cerff et al., (2012) had proved the magnetophoretic separation of marine microalgae from seawater but without the detailed study on the nature of interaction(s) involved. Supposedly, the ionic stress induced by high salt concentration in seawater would cause retardation of inter-particles Debye screening length, and hence inhibit the electrostatic attraction between the cells and magnetic particles (Yeap et al., 2012a). Thus, the interaction scheme that induces the particle-to-microalgal cell attachment in seawater condition is yet to be explored. Good understanding on the fundamental knowledge is important to drive the future improvement and development of this technology. Therefore, mechanistic study onto the raw material characterization, the interaction that promote effective cell separation, and the feasibility of this method onto the fishpond water treatment and biofuel production purpose should be clearly verified. Furthermore, the identification on the feasibility of this method on fishpond water treatment through the real engineering application demonstration was needed in order to address the feasibility and effectiveness of this approach. Moreover, the

cost analysis study on the fishpond water treatment and biofuel production is desired to figure out the engineering potential of magnetophoretic separation for microalgae separation.

1.6 Research Objectives

The main objective of this thesis is (1) to enable the magnetophoretic separation of microalgae from their liquid suspension without the need of pH adjustment after imparting a magnetic property onto the microalgal cells and (2) to study the fundamental and feasibility aspect of microalgae harvesting through low gradient magnetophoretic separation (LGMS). The specific objectives are as below:

- i. To surface functionalize the iron oxide nanoparticles (IONPs) with cationic polyelectrolyte to form a colloiddally stable and positively charged magnetic nanoparticles.
- ii. To study the nature of particle-to-microalgal cell interactions involved when in freshwater and seawater, by using Extended Derjaguin-Landau-Verwey-Overbeek (XDLVO) analysis, which dictate the successful application of magnetophoretic separation for harvesting microalgal cells.
- iii. To characterize both the transient (the separation kinetic) and spatial behaviour of LGMS in magnetophoretic separation of microalgal cells.
- iv. To verify the critical parameters which influence the efficiency of the magnetophoretic separation of microalgae.
- v. To demonstrate the effectiveness and feasibility of the magnetophoretic separation method for real environmental system application and also for biofuel production.

1.7 Scope of Study

Positively charged IONPs was developed in order to enable the attachment of IONPs on the surface of microalgae in freshwater through the promising electrostatic-mediated-attachment mechanism. The positively charged IONPs without having isoelectric point tend to avoid the need of pH adjustment onto the huge volume of microalgal suspension and also able to ensure the quality of the biomass and supernatant/treated water. Hence, magnetophoretic separation will become practical in real engineering application.

Next, interaction between the IONPs and microalgal cells was modeled in order to understand the underlying mechanism involved which leads to the attachment of IONPs. By having this information, the effectiveness of the particle-to-microalgal cell attachment becomes predictable without the need of laborious experimental study. Moreover, the way to detach the IONPs from the harvested biomass was being explored too in order to reuse the IONPs.

The effectiveness study was carried out to investigate the parameters which intend to affect the efficiency of the magnetophoretic separation of microalgae. The parameters considered were the property and character of the IONPs, dosage of IONPs, and the different species of microalgae. Therefore, the limitation on the separation performance can be investigated and the feasibility of this separation technology onto wide range of microalgae medium can be confirmed.

Besides that, the quality of the harvested biomass and the supernatant/treated water were investigated in order to demonstrate the feasibility of magnetophoretic separation method for biofuel production purpose and also for water treatment.

Lastly, a cost analysis on the water treatment and also the biofuel production by magnetophoretic separation technique was carried out in order to identify if this technology is promising. An overview of the scope of study is outlined in Figure 1.1.

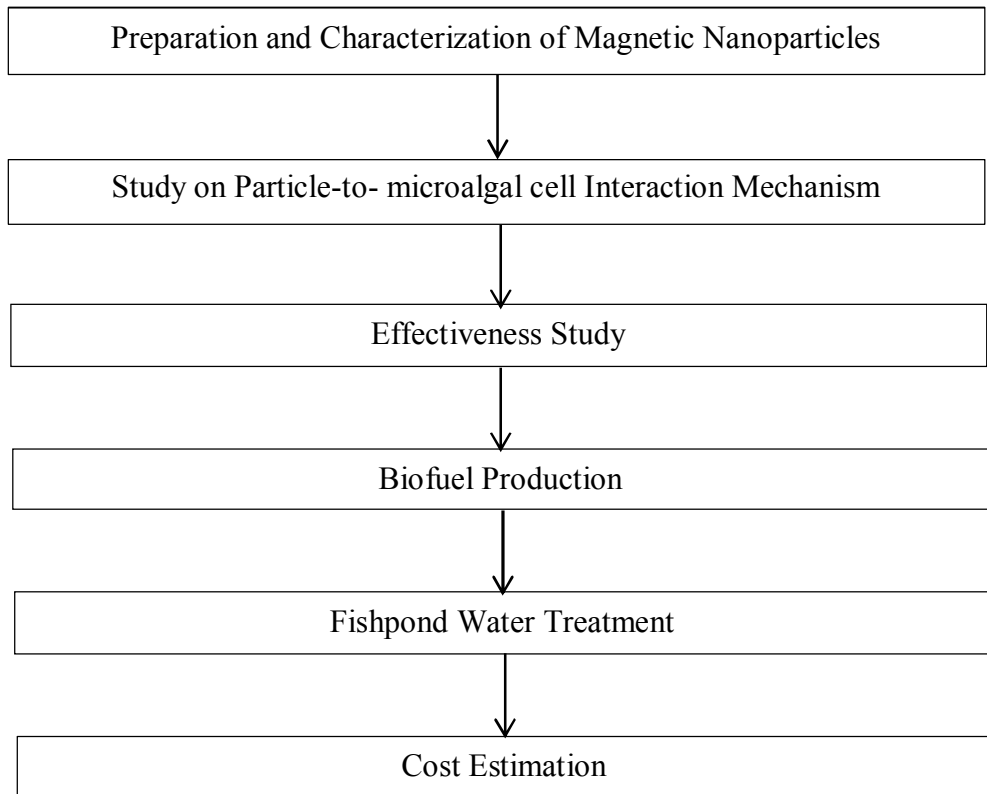


Figure 1.1: Schematic flowchart of the scope of study.

1.8 Organization of Thesis

This thesis consists of five chapters, where each of these chapters is summarized as below:

Chapter one gives the introduction on the problem of microalgae blooming in the nutrient rich pond water of aquaculture and fishfarm, the potential of harvested microalgae biomass as the feedstock of biofuel, the conventional method of microalgae harvesting, and the description on the magnetophoretic separation method that proposed for present study. The problem statement reveals the weakness of the magnetophoretic separation method until current stage of study together with

its limited information allowing its full industrial application. The objectives of this research were listed out with the aim to mitigate the existing weakness and explore the fundamental aspect of this separation technology. Latter the feasibility study in term of cell separation efficiency, workable on real fishpond water treatment, and its potential on biofuel production purpose were carried out.

Chapter two reviews the concept of magnetophoretic separation of microalgae and the biofuel production. The literature review starts with the review on characteristic of magnetic nanoparticles and cationic polyelectrolytes, the methods and the importance of surface functionalization on magnetic nanoparticles, and the importance and the mechanism to maintain colloidal stability. The underlying principle which governs the interaction between the microalgal cells and magnetic nanoparticles are discussed. Furthermore, the type of separators, the satisfaction on the quality of microalgal biodiesel, the toxicity of magnetic nanoparticles, and also the methods of biodiesel preparation has been included.

All the experimental materials and methods used throughout this study were presented in chapter three. The detailed information of the required chemicals and laboratory apparatus for the preparation and characterization of magnetic nanoparticles, characterization of microalgae, cell separation experiments and other relevant experiments are presented together with clear description on the experimental procedure.

Chapter four encompasses all the experimental results together with detailed discussion. The discussion begins with the characterization of the magnetic nanoparticle that proposed for present study. Then, the interaction mechanism of particle-to-microalgal cell and its kinetic separation under low gradient magnetic field was investigated. The interaction of particle-to-microalgal cell was modeled by

XDLVO analysis together with detailed description. This chapter was followed by in-depth discussion on four critical parameters that significantly affect the performance of existing separation method. The following section discussed the feasibility of magnetophoretic separation method onto the fishpond water treatment and biofuel production. Lastly, the potential of the application of present separation technology on fishpond water treatment and biofuel production was discussed base on the cost estimation.

In chapter five, the whole studies and findings in this research was concluded and followed with some recommendations for future study.

CHAPTER TWO

LITERATURE REVIEW

In this chapter, the modification of the magnetophoretic separation of microalgae from 1970s until now is illustrated and followed with the review on mechanism of attachment of IONPs on cells and also the model system employed to describe the interaction quantitatively. Next, the characteristic of different type of iron oxide magnetic nanoparticles (IONPs) are presented first. Then, the different ways to surface functionalize the IONPs and the commonly employed cationic polyelectrolytes in environment are reviewed. The discussion about the mechanism to induce colloidal stability on IONPs and its advantages are included. Furthermore, the design and performance of magnetic separators are described. Moreover, the satisfaction of microalgal biodiesel to compete with crude diesel in term of oil quality and price, toxicity of IONPs, and the methods of biodiesel preparation from microalgal biomass are enclosed.

2.1 Characteristic of Microalgae

One of the freshwater microalgae strains that can easily found in surrounding water body is the *Chlorella* sp. (Belcher and Swale, 1976). The *Chlorella* sp. microalga is a common genus of green algae that has been widely used as model for studies because it is easily to grow in laboratory and outdoor in rapid manner (Tate et al., 2012). It is a small round or oval cells with typical diameter in range of 2-15 μm and will divide into two or four daughter cells during cell division (Belcher and Swale, 1976). The oil content of *Chlorella* sp. is at 28-32 % of dry weight which is a potential biodiesel feedstock (Chisti, 2007).

Besides in freshwater, microalgae also can found abundantly in seawater. The unicellular green alga *Nannochloropsis* sp. is a marine microalga which is a potential biofuel feedstock due to high production of triacylglyceride (Vieler et al., 2012). It contains high oil content at 31-68 % dry weight (Chisti, 2007). *Nannochloropsis* sp. is belonging to Eustimatophyceae in small size around 2-3 μm and growing fast under photoautotrophic condition (Anandarajah et al., 2012; Mitra et al., 2015). It is an efficient carbon-fixing agent to combat with the global warming by sequestering of CO_2 (Mitra et al., 2015). Besides that, the marine diatom *Amphora* sp. also found abundant in oceans, especially in upwelling area likes coastal and open ocean. Diatom as one of the classes of microalgae from Bacillariophyceae (Gaiser, 2004; Lane et al., 2009) which have higher growth rates than other algae of corresponding size. They are unicellular, eukaryotic and photosynthetic microalgae (Prestegard, 2009). Moreover, diatoms are the dominant life form in phytoplankton and are of crucial importance in marine systems from an ecological and biogeochemical point of view (Allen, 2006; Demirbas, 2010). One of the unique characteristic of the diatoms *Amphora* sp. is that they have silica cell wall called frustules and they produced extracellular polymeric substances (EPS), which mainly composed of carbohydrates with a small fraction of proteins, during growth (Zhang et al., 2008). The available of EPS on diatom *Amphora* sp. has caused their surface property different from other microalgae.

Generally, open pond is the most common and simple systems that can found easily in our surrounding where the microalgae are growing naturally and autotrophically under sunlight and consume the carbon dioxide (CO_2) from atmosphere (Chen et al., 2010). However, the cell density of microalgae cultivated in open pond can only reach to as high as 1 g/L. The harvesting of those micron-size

microalgae from the huge volume of water system but in low cell density is quite challenging. Therefore, several methods to separate the microalgae from water have been developed due to their unique properties.

2.1.1 Conventional Method on Microalgae Separation

There are several well developed methods that are commonly used for microalgae separation. They are centrifugation, filtration and the flocculation and settling. Centrifugation is the most reliable method with rapid biomass separation (Molina-Grima et al., 2003). However, it is expensive, high energy consumption, and high maintenance requirement due to the moving parts (Lee et al., 2009; Kim et al., 2013). It is not suitable to handle enormous quantity of effluents but only suitable for high value product (Yadida et al., 1997; Brennan and Owende, 2010). Filtration method has recorded high separation efficiency, simple, enable continuous operation and also no requirement of chemical (Kim et al., 2013). However, this method is quite costly with the fouling and clogging problem and in low throughput (Hoffmann, 1998; Molina-Grima et al., 2003; Mata et al., 2010). This method is only suitable for relatively large, filamentous or colony forming microalgae rather than the microalgae approaching bacterial dimensions (Molina-Grima et al., 2003; Lee et al., 2009). Flocculation and settling is a cost effective and versatile method that is suitable to process large quantity of biomass (Vandamme et al., 2013). This method has been commonly used for water treatment and sludge dewatering purpose. However, the performance of this method is relying on the selection of flocculant. For example, the use of multivalent metal salts as flocculant tend to contaminate the microalgal biomass (Vandamme et al., 2013) while the efficiency of the cationic polymer will be inhibited by the high ionic strength of seawater (Bilanovic et al., 1988). Moreover,

the harvested biomass is dilute and in high moisture content, which is undesired because the downstream drying process will become costly (Molina-Grima et al., 2003). This method is time consuming too (Nurdogan and Oswald, 1996). Due to the various drawbacks and weakness found from these harvesting methods, the invention and discovery on the new method of microalgae harvesting is continued in order to meet an efficient and cost effective harvesting strategy. Therefore, the method of magnetophoretic separation of microalgae is being recalled due to its advantages against the conventional methods.

2.1.2 Magnetophoretic Separation of Microalgae

The method of magnetophoretic separation of microalgae from pond water was being investigated since 1970s in purpose to treat the algae bloomed lake water so that the eutrophication problem can be solved (Bitton et al., 1975). Before that, the flocculation method used to harvest the microalgae was recognized as more economic than the centrifugation method (Yadidia et al., 1977). However, the high gradient magnetophoretic separation (HGMS) had been proved suitable for water pollution control after seeded the pollutant with magnetite because it enabled the high processing capacity (De Latour, 1973). Therefore, the experimental studies on microalgae harvesting through HGMS with the aided of flocculation that has seeded with magnetic particles was carried out to identify its feasibility on lake water treatment (Bitton et al., 1975) while also enabled the biomass recovery (Yadidia et al., 1977).

In HGMS, the microalgae sample is seeded with the magnetic particles. Then the metallic salts flocculant, such as aluminum sulfate or alum, $\text{Al}_2(\text{SO}_4)_3 \cdot 18\text{H}_2\text{O}$, or the ferric chloride, FeCl_3 , was mixed with the suspending microalgal cells and

magnetic particles for duration of more than 5 min to form magnetized flocs. Hence, the flocculated mixture was then poured through the high gradient magnetic separator (Bitton et al., 1975; Yadidia et al., 1977). This separation process mimics the filtration method where the magnetized flocs were retained in the magnetized wool matrix while left over the clean supernatant to pass through the wool matrix and been collected. Ying et al (2000) reported that the filtration effect had contributed 30% in the removal efficiency of the polystyrene particles when no magnetic field. Hence, the HGMS in those studies was being named as high gradient magnetic filtration (HGMF) (Bitton et al., 1975; Yadidia et al., 1977).

From the study of Bitton and co-workers, they were performing the HGMF onto the sample from the Florida lakes by using alum as the flocculant and seeded with magnetic particles. The efficiency of microalgae removal was relied on the water pH because the performance of alum was pH dependent. Hence, the sample was being adjusted from pH > 8.5 to pH 6.5 in order to yield high cell removal efficiency (> 80 %) after mixed with 300 mg/L of magnetic particles (Bitton et al., 1975). On the other hand, Yadidia and co-workers (1977) were preferred the ferric chloride rather than the alum due to the reason of the ferric chloride produced more resilient and less toxic flocs. However, the pH of the algae sample needs to be adjusted to an even lower pH value of 4 for ferric chloride to perform well. Even with the aid of ferric chloride flocculant, the dosage of magnetic particles that needed to achieve 90 % of *Scenedesmus obliquus* algae separation from the pond medium was at about 39 g magnetic particles per g of biomass initially was drastic increased to 167 g magnetic particles per g of biomass in order to achieve 95 % of separation efficiency (Yadidia et al., 1977). From the above review, both studies shared the similar drawback that is the need of pH adjustment onto the microalgae sample in

order to make the HGMF efficient. It is not practical for real environmental water treatment since huge volume of acid are needed to adjust the pH of lake water and also the acidic supernatant released tend to threaten the aquatic life, especially in the case where ferric chloride is used. Therefore, this method needs to be improved.

In 2000s, the method of microalgae separation through magnetophoresis was being re-visited. Besides the water treatment purpose (Liu et al., 2009), it was being considered as a potential harvesting method for biofuel feedstock production too (Xu et al., 2011; Wang et al., 2013b). Liu and co-workers were use the similar flocculation-aided magnetophoretic separation method of Bitton et al. (1975) and Yadidia et al. (1977) to remove the microalgae (*Microcystis aeruginosa*) from the water of Chaohu Lake (Hefei, China). They had replaced the metallic salts flocculant with polymeric flocculant, chitosan, which was biodegradable and also the used of nano-sized magnetic particles (Liu et al., 2009). They found that the cell separation efficiency was achieved up to 99 % at pH 7 in particle dosage of about 8×10^{-10} mg magnetic particles per cells, which was far more lower dosage compared to the work of Bitton et al. (1975) at about 3.8×10^{-6} mg magnetic particles per cells. This comparison has proved that the smaller size of magnetic particles induce better cell separation efficiency, which was also proved by Yadidia et al. (1977).

In order to retain the high specific surface area of nanoparticles to induce higher cell separation efficiency, there are a number of studies on the direct attachment of magnetic nanoparticles onto the microalgal cells without the aid of flocculation process (Cerff et al., 2012; Xu et al., 2011; Hu et al., 2013; Lee et al., 2013; Seo et al., 2013). They had performed the direct attachment method through different interaction mechanism and self-designed magnetic particles, which will be discussed in following section 2.2.2(a).

2.1.2(a) Interaction Mechanism

There are two type of interaction mechanisms use to induce the attachment of particle-to-microalgal cell that are the adsorption-based-attachment (Cerff et al., 2012; Hu et al., 2013) and electrostatic-mediated-attachment (Xu et al., 2011; Prochazkova et al., 2013; Lee et al., 2013; Seo et al., 2014). The extent of the successful attachment of particle-to-microalgal cell is presented in cell separation efficiency.

For the adsorption-based-attachment interaction mechanism, the attachment of particle-to-microalgal cell is mainly affected by the particle and cell surface property and also the cultivation medium components. From the study of Cerff et al. (2012), the hydrophilic silica-coated magnetic particles in micron-size (5 μm and 9 μm) has enabled the removal of freshwater *Chlamydomonas reinhardtii* cell from different type of culture medium at > 90 % when in particle dosage higher than 0.07 g magnetic particles/g biomass. The attachment of particle-to-microalgal cell was effective even though both surfaces were in negative charge. The affective attachment of particle-to-microalgal cell might be initiated by another form of adsorption beside the electrostatic (ES) interaction. For the case of freshwater *Chlorella vulgaris*, the effectiveness of attachment was depended on different type of culture medium, where the cell separation efficiency in IGV-medium and modified TAP-medium are 95 % and 20 % respectively. The concentration of Mg^{2+} in the IGV-medium is fivefold higher compared to the modified TAP-medium was being suspected as the reason that promote high cell separation. For the test on marine species *Phaeodactylum tricornutum*, the high cell separation was achieved at efficiency of 95 % due to its adhesive surface property; while for the marine

Nannochloropsis salina, it was only being separated at high pH condition ($\text{pH} \geq 10$) which promote flocculation (Cerff et al., 2012). On the other hand, Hu and co-workers had proved that the magnetic nanoparticles without and with the coating of polyethylenimine (PEI) were successfully attached on the cell surface through nano-size adsorption with ≥ 95 % of cell separation efficiency was achieved (Hu et al., 2013; Hu et al., 2014a).

For the electrostatic-mediated-attachment, the interacting surfaces must be in opposing charge. Normally, the microalgal cells are negatively charged (Molina-Grima et al., 2003; McLaughlin and Poo, 1981; Kinraide et al., 1992; Gadd, 2009). Hence, the positively charged magnetic particles are desired to form effective attachment through ES attraction. In order to prove the interaction of particle-to-microalgal cell is mediated by the ES attraction, the test on the separation of microalgal cell in different pH condition was carried out (Xu et al., 2011; Prochazkova et al., 2013). The cell separation efficiency was in accordance with the surface charge on the magnetic particle with respect to the pH. Xu and co-workers (2011) proved that the bare-IONPs, with an isoelectric point at pH 6.8, were in negative charge when dispersed in the cell medium at pH 7. It enabled the separation of *Chlorella ellipsoidea* cells from the natural cell medium because the *C. ellipsoidea*, with an isoelectric point at pH 7.5, was having an opposing charge to the bare-IONPs. However, it failed to remove the *Botryococcus Branuii* cells from the medium because the bare-IONPs has a very low surface charge density when in the cell medium at pH 7. In order to induce the separation of *B. Branuii*, higher dosage of magnetic particles was required, at about 0.042 g magnetic nanoparticles/g biomass, compared to that at pH 4, with only half of the dosage at pH 7 was needed to achieve 99 % of cell separation efficiency (Xu et al., 2011). Prochazkova and co-workers

(2013) had surface functionalized the IONPs with different polyelectrolyte to form surface functionalized iron oxide magnetic nanoparticles (SF-IONPs). The surface property of SF-IONPs takes the property of the polymer layer that coated on it. They showed that the SF-IONPs coated by diethylaminoethyl (DEAE), with an isoelectric point at pH 6.3 lower than the pH of cell medium, required 3 times higher dosage of SF-IONPs to achieve 95 % of cell separation compared to the acidic condition ($\text{pH} \leq 4$) (Prochazkova et al., 2013). This finding was similar with the case of Xu et al. (2011). Therefore, the selection of polyelectrolyte is important to ensure the effective attachment of magnetic particles on cell surface at the natural pH condition of cell culture. Furthermore, the pH adjustment on the cell medium is highly prohibited due to the huge volume of water. The summarized cell separation efficiency together with the interaction conditions were illustrated in Table 2.1.

According to the above point of view, the electrostatic-mediated-attachment is predictable according to the determination of isoelectric point of each interacting surfaces. Moreover, the detachment of the magnetic particles from cell surface is also predictable if the effective attachment of particle-to-microalgal cell is through the ES attraction. The detachment is important to recover the magnetic particles for reuse in, where it was always carried out at pH 12 (Prochazkova et al., 2013; Seo et al., 2014). At pH 12, the magnetic particles with a lower isoelectric point will become negatively charged that is similar with microalgal cells. Then, the ES repulsion force will generate between the cells and particles to induce detachment. Prochazkova and co-workers showed that the detachment of magnetic beads (0.5 μm) can achieved up to 90 % efficiency (Prochazkova et al., 2013) while Seo and co-workers showed that the detachment of barium ferrite was achieved up to 85 % of efficiency when in size of 1.2 μm but weak detachment (12.5 %) on the nano-size particles (108 nm) (Seo et

al., 2014). This detachment method is seems applicable for micron-size magnetic particles while not effective for nanoparticles.

On the other hand, Xu and co-workers had suggested another way to regenerate the magnetic particles. They chose to dissolve the particle-attached-microalgal cell by hydrochloric acid (HCl) and followed with micro-filtration to remove the cells. The filtrate was used to synthesize the iron oxide again (Xu et al., 2011). This method is applicable due to the excellent separation efficiency of microalgae has maintained after reuse for five times. However, the direct detachment of the magnetic particles from the cell surface for reuse seemes more attractive and economic.

Table 2.1: Cell separation performance in different case studied.

Materials	Cell sample	Cell separation efficiency (%)	Particle dosage (g/g)*	pH of cell medium	References
Flocculation-aided magnetophoretic separation method					
Magnetite and Alum	Sample from Clear Lake	>80%	- (3.8x10 ⁻⁶)**	Adjusted to pH6.5	Bitton et al., 1975
Magnetite and Ferric chloride	Pond effluent algae	90%	39	Adjusted to pH4	Yadidia et al., 1977
Ferroferric oxide and Chitosan	Sample from Chaohu Lake	99%	- (8x10 ⁻¹⁰)**	7	Liu et al., 2009
Adsorption-based-attachment mechanism					
Silica-coated magnetic particles (5µm and 9µm)	<i>C. reinhardtii</i> WT08	99%	0.07	8	Cerff et al., 2012
	<i>C. reinhardtii</i> WT13	90%	0.3	8	
		99%	1.4		
	<i>C. vulgaris</i> (IGV medium)	95%	3	8	
	<i>C. vulgaris</i> (Modified TAP medium)	≤20%	7	8	
	<i>P. tricornutum</i> ***	95%	0.6	8.1	
	<i>N. salina</i> ***	<45%	4.5	8	
Bare-IONPs (10nm)	<i>N. maritime</i> ***	90%(Flocculation)	0.2	Adjusted to pH10	
IONPs coated with PEI (12nm)	<i>C. ellipsoidea</i>	>95%	0.1	8	Hu et al., 2013
		95%	0.03	9	Hu et al., 2014a
Electrostatic-mediated-attachment mechanism					
Bare-IONPs (10nm; pI = pH6.8)	<i>B. braunii</i> (no pI)	99% (Adsorption)	0.042	7	Xu et al., 2011
	<i>C. ellipsoidea</i> (pI = pH7.5)	99%	0.375	7	
Magnetic bead coated with DEAE (0.5µm; pI = 6.3)	<i>C. vulgaris</i> (no pI)	95% (Adsorption)	0.8	7	Prochazkova et al., 2013
	Magnetic bead coated with PEI (0.5µm; pI = 8.9)	95%	0.27	7	
IONPs coated with chitosan (10-30 nm)	<i>Chlorella</i> sp. KR-1	99%	1.4	6.90±0.16	Lee et al., 2013
Barrium Ferrite coated with APTES (pI = 9.85)	<i>Chlorella</i> sp. KR-1	≥98.6%	-	7	Seo et al., 2014

*The unit of g/g represents the g magnetic particles/g biomass. **Unit: mg magnetic particles/cell. ***Marine strain of microalgae.